Cerebral Cortex April 2007;17:918-928
doi:10.1093/cercor/bhl002
Advance Access publication May 24, 2006

Modulation of Visual Responses in Macaque Frontal Eye Field during Covert Tracking of Invisible Targets

Quan Xiao, Andrei Barborica and Vincent P. Ferrera

Department of Psychiatry, Center for Neurobiology and Behavior, David Mahoney Center for Brain and Behavior Research, Columbia University, New York, NY 10032, USA

The purpose of this study was to investigate the interaction between internal representations of invisible moving targets and visual responses of neurons in frontal eye fields (FEFs). Monkeys were trained to make saccades to the extrapolated position of a target that was temporarily rendered invisible for variable durations as if it had passed behind an occluder. Flashed, task-irrelevant visual probe stimuli were used to study the visual responsiveness of FEF neurons during this task. Probes were flashed at various times and locations during the occlusion interval. Net changes in neuronal activity were obtained by comparing the activity on trials with probes with randomly interleaved trials without any probe. Most neurons showed an increase in firing rate in response to the probe, but some showed a decrease. Both types of responses were enhanced when the invisible target moved toward the receptive field (RF) as compared with trials on which the target moved away from the RF. Some neurons showed a spatial shift in the visual response during the occlusion interval. For cells that were excited by the probe, the shift tended to be correlated with the direction of motion of the target, whereas for cells that were inhibited the shift tended to be in the opposite direction. These results suggest that the role of FEF in predicting invisible target motion includes a sensory/perceptual component.

Keywords: frontal eye field, monkey, motion, prediction, saccade

Introduction

Monkeys and humans can predict the future location of a moving target that is made temporarily invisible (Rosenbaum 1975; Pavel and others 1992; Filion and others 1996). This ability has been termed "representational momentum" (Freyd and Finke 1984; Kelly and Freyd 1987) and may be a rudimentary form of object permanence (Piaget 1954; Watson and others 2001; Churchland and others 2003). Humans can track invisible moving targets using a combination of smooth pursuit and saccadic eye movements for up to 1200 ms (Bennett and Barnes 2006; Orban de Xivry and others 2006). The ability to predict motion is impaired in schizophrenia patients (Hooker and Park 2000), suggesting a possible link to prefrontal pathology (Goldman-Rakic and Selemon 1997). Currently, little is known about the role of prefrontal cortical areas such as the frontal eye fields (FEFs) in producing this behavior. FEF is part of a fronto-parietal attention network (Posner and Petersen 1990) and is directly involved in the planning and execution of voluntary eye movements (Ferrier 1876; Bruce and Goldberg 1985; Bruce and others 1985). Neurons in the FEF exhibit spatially selective responses to the presentation of visual targets as well as during preparation and execution of saccadic and smooth eye movements. Previous work in our lab has suggested a role for FEF in predicting target motion (Barborica and Ferrera 2003, 2004) but has not indicated whether this role involves modulation of visual responses as opposed to movement-related activity.

The ability to predict the future location of a moving target may involve the active deployment of visual attention along the target trajectory (Barborica and Ferrera 2004). Neuronal sensitivity to visual stimuli in primate FEF may be an index of visual–spatial attention (Moore and Fallah 2001; Moore and others 2003). Spatial attention can shift receptive fields (RFs) in visual cortex (Connor and others 1997). Visual responses in FEF can be enhanced for stimuli that are the target of a saccade (Goldberg and Bushnell 1981). Visual RFs may also shift predictively around the time of a saccadic eye movement (Goldberg and Bruce 1990; Umeno and Goldberg 1997). The motivation for this study was to investigate whether visual responses in FEF are either enhanced or spatially shifted when monkeys make predictive saccades to the future location of a moving visual stimulus. If visual responses are modulated (either enhanced or shifted) during the task, this would provide evidence that an internal representation of moving targets in FEF has a sensory/perceptual component.

Methods

Experiments were performed on 5 male subadult rhesus monkeys (*Macaca mulatta*). The treatment of the monkeys was in accordance with the guidelines set by the US Department of Health and Human Services (National Institutes of Health) for the care and use of laboratory animals, and all methods were approved by the Institutional Animal Care and Use Committee at Columbia University and the New York State Psychiatric Institute. Monkeys were prepared for experiments by surgical implantation of a post for head restraint and a recording chamber to give access to the cortex. Eye position was recorded using a monocular scleral search coil (Judge and others 1980). All surgical procedures were performed using aseptic technique and general anesthesia (1–3% isoflurane). Monkeys were trained to sit in a primate chair for the duration of each experiment with their heads restrained. Correct performance was reinforced by liquid reward.

Visual Stimuli and Display

Visual stimuli were generated and controlled by a Cambridge Research Systems VSG2/3F video frame buffer. The output from the video board was displayed on a calibrated 29- or 37-inch color monitor (Mitsubishi) with a 60-Hz noninterlaced refresh rate. The monitor stood at a viewing distance of 61 or 76 cm (depending on monitor size) so that the display area subtended roughly 40 degrees horizontally by 30 degrees vertically. The spatial resolution of the display was 1280 × 1024 pixels. The central fixation point was a small (0.5 degrees) white square presented on a uniform black background. The luminance of the fixation target was 65 cd/m^2, whereas the background was the minimum luminance (0 cd/m^2, below the photometer threshold). Moving targets were small gray discs (1 degree in diameter, luminance 32 cd/m^2) that moved either toward or away from the neurons' RFs. Visual probes were small yellow squares (0.7 degrees, 32 cd/m^2).

Eye Movement Recording

Eye movements were recorded using a scleral search coil system (CNC engineering). Horizontal and vertical eye positions were sampled at

1 kHz per channel and digitized with 12-bit resolution. The times of saccade onset and offset on each trial were identified using an acceleration criterion (radial eye acceleration $\geq$ 500 degrees/s^2 for onsets or $\leq$ 500 degrees/s^2 for offsets). Individual trials were inspected visually to make sure that small saccades did not go undetected.

Neuronal Recording and Electrical Stimulation

A recording chamber (20-mm diameter) was implanted on the skull overlying the arcuate sulcus. The recording chamber was positioned at stereotaxic coordinates 25A, 15L (Paxinos and others 2000). At the start of each recording session, a hydraulic microdrive was mounted on the recording chamber. Recordings were made using platinum–iridium or tungsten electrodes with impedances of 0.3–2 Mohm at the rate of 1 kHz. Signals from the microelectrode were amplified, filtered, and monitored on an oscilloscope and audio monitor. A time–amplitude window discriminator converted extracellular action potentials into digital pulses which were sampled by the computer with 0.01-ms time resolution. Units were isolated on the basis of waveform. Neuronal spike trains were collected and stored along with eye position and velocity records.

Electrical microstimulation was used to map the region of cortex from which neuronal recordings were obtained in each monkey. Sites in periarcuate cortex were stimulated through the same electrode used to record neuronal activity. The stimulation consisted of a train of 0.2 ms biphasic pulses at a rate of 350 pulses/s delivered by an optically isolated pulse stimulator (AM Systems, Carlsborg, WA). The output of the stimulator was gated by a computer-generated digital signal level so as to be synchronized with other trial events. The current threshold for evoking saccades was determined by stimulating during a fixation task (Opris and others 2001). The threshold was defined as the current level at which involuntary saccades were evoked on about half the stimulation trials (Bruce and others 1985). For 284 periarcuate sites the median threshold was 42.5 μA (min 10 μA and max 100 μA). Further details regarding the physiological and anatomical characterization of recording sites can be found in previous papers (Opris and others 2005).

Behavioral Paradigms

Monkeys were trained to perform 2 tasks during neuronal recording. One was a memory saccade task (MEM). Another was a motion extrapolation task to estimate invisible target's position (PREDMAP). The MEM task was used to the preferred spatial location for each cell and to identify visual and movement-related activities. The PREDMAP task was used to map visual responses while the monkey planned saccades to the future location of an invisible moving target.

In the MEM task, monkeys made saccades to the remembered location of a stationary visual cue. The cue location varied among 8 positions, equally spaced (45 degrees) around the clock (Fig. 2*A*, Funahashi and others 1989). At the beginning of each trial, the monkey fixated a small white square. A peripheral cue was flashed for 750 ms followed by a variable delay (750–1250 ms) during which the fixation target remained on, and the monkey maintained fixation within a 2 × 2-degree window. At the end of the delay, the fixation target disappeared, and the monkey was allowed up to 800 ms to make a saccade to the remembered location of the cue. After the 800-ms saccade interval and if the monkey's memory saccade was within a 3 × 3-degree window centered on the cue location, the cue reappeared to provide feedback to the monkey, and corrective saccades were generally made at this time. The eccentricity of the peripheral cue was varied to find the optimum eccentricity for each neuron before data were recorded. Data were then recorded with this fixed eccentricity.

In the PREDMAP task (Fig. 1), the monkey maintained fixation within a 2 × 2-degree window centered around the fixation target. A moving target was then presented in the periphery and moved for 750 ms along a trajectory that was either toward or away from the neuron's RF. The target then disappeared as if it has passed behind an occluder. The monkey was required to maintain fixation for a variable delay interval. Then the fixation point was turned off, which served as the GO signal for the monkey to initiate a saccade to the extrapolated position of the invisible target. If the saccade end point was within a 5 × 5-degree window centered on the position of invisible target, the monkey received juice as reward. For any given recording site, 2 opposite

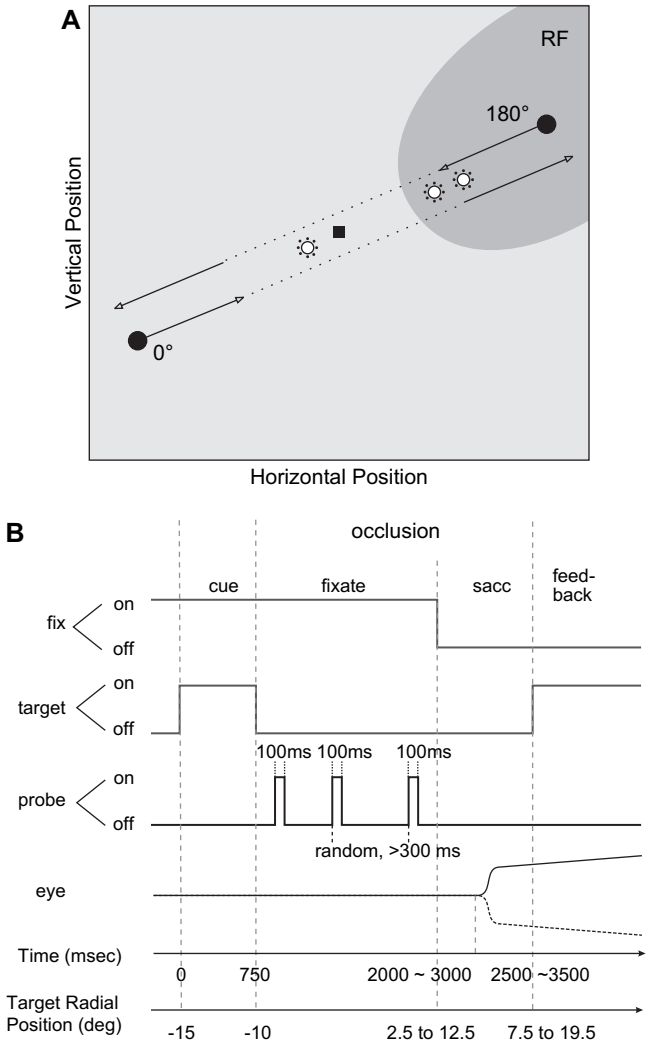

Figure 1. Behavioral paradigm for PREDMAP task. (*A*) Target (black circles) moves either toward or away from the RF (dark gray region). The target paths for the 2 directions of motion are separated for clarity. In the actual experiment, they overlapped with each other and with the locations of the fixation point (black square) and probe stimuli (white circles). (*B*) Event timing during task. The moving target was initially visible for 750 ms. Then it was invisible for a 1.75- to 2.75-s occlusion interval, the first 1.5–2.25 s of which preceded the GO signal to make the saccade. The monkey was allowed up to 500 ms to initiate the saccade, after which the target reappeared. Probes were flashed for 100 ms with a minimum of 300 ms between the onsets of successive probes.

directions of target motion were used. However, the orientation of the target path was adjusted for each site. Over the entire set of recording sites, the target motions used covered a full 360-degree range. Likewise, the target speed was constant for any given site but varied across sites in the range of 6–14 degrees/s. Visual probe stimuli consisting of 0.7 × 0.7-degree yellow squares were presented in some trials. The probe duration was 100 ms. The number of probes on any given trial was between 1 and 3. The minimum time between the onsets of successive probes was 300 ms. Over different trials, probes were presented at 16 locations along the target path and at 7 different times relative to the onset of the occlusion interval (112 combinations). Monkeys were given feedback regarding the accuracy of their saccade by making the target visible again after the saccade. As a control, trials with no probe were randomly interleaved with probe trials.

Statistics

To estimate linear relationships between 2 variables, correlation coefficients and regression lines are computed. Correlation is computed

using Pearson's *r*. For best-fitting linear regression lines, the standard method is to minimize the vertical distance to the regression line. However, this method produces systematic biases when there is random variability in both variables (the slope is underestimated, whereas the intercept is overestimated). We therefore use principal components regression. This method involves computing the principal components of the data and using the first principal component for the slope and intercept of the regression line.

Results

We recorded the activity of 191 neurons at 127 recording sites in the saccade subregion of the FEFs from 5 monkeys (monkey A $n = 24$; C $n = 6$; D $n = 18$; E $n = 21$; F $n = 122$) while monkeys performed the PREDMAP task. The majority (135/191) of neurons were also tested with the MEM task, to determine the location for RF of that unit and to compare the relative strength of the visual cue interval and presaccadic interval. Once the RF of the neuron was determined, the target path for the PREDMAP task was rotated to be aligned with the RF for that cell. Cells without MEM recordings ($N = 56$) were always adjacent to cells with MEM recordings. That is, they were recorded on the same electrode or on separate electrodes whose tips were less than 50 μm apart. Because FEF is topographically organized and has a columnar organization, neighboring units tend to have similar RFs. We found that 122 (64%) neurons responded best to visual stimuli in the contralateral visual field, 50 (26%) in the ipsilateral field, and 19 (10%) on the vertical meridian.

Behavioral Performance

The PREDMAP task required the monkey to estimate the position of an invisible target that moved in 1 of 2 directions, either toward or away from the location of the neuron's RF. The behavioral measure was the eye position at the end of the first saccade initiated after the GO signal and before the reappearance of the target. The accuracy with which the monkey estimated invisible target position was quantified by calculating the 2-dimensional (2D) correlation coefficient between eye position and target position at the time when the saccade ended. The 2D correlation was computed by representing saccade end point (s) and target position (t) on each trial as a complex number ($x + yi$). The correlation was then computed using Pearson's formula. Figure 2*A* shows the correlation of invisible target position and saccade end point for one recording session. Figure 2*B* shows the distribution of the correlation coefficients for all 127 recordings, split by target direction for a total of 254 measurements. The mean ± standard deviation (SD) of the distribution was 0.34 ± 0.15. This performance is comparable with that reported in previous work from our lab (Barborica and Ferrera 2004). Factors that may degrade the monkeys' performance are the large spatial and temporal intervals over which occlusion occurs as well as the potentially distracting effect of the visual probes. However, when trials were split depending on the presence or absence of probe stimuli, there was no significant difference between the correlation coefficients for probe and no-probe trials (paired *t*-test; $P = 0.24$).

The 2D correlation uses all the information about saccade end point and target position but is difficult to visualize because the data occupy a 4D space. A simpler method is to reduce the saccade end points and target positions to one dimension apiece. This was done by calculating the eccentricity of the saccade end point and target position using the Pythagorean

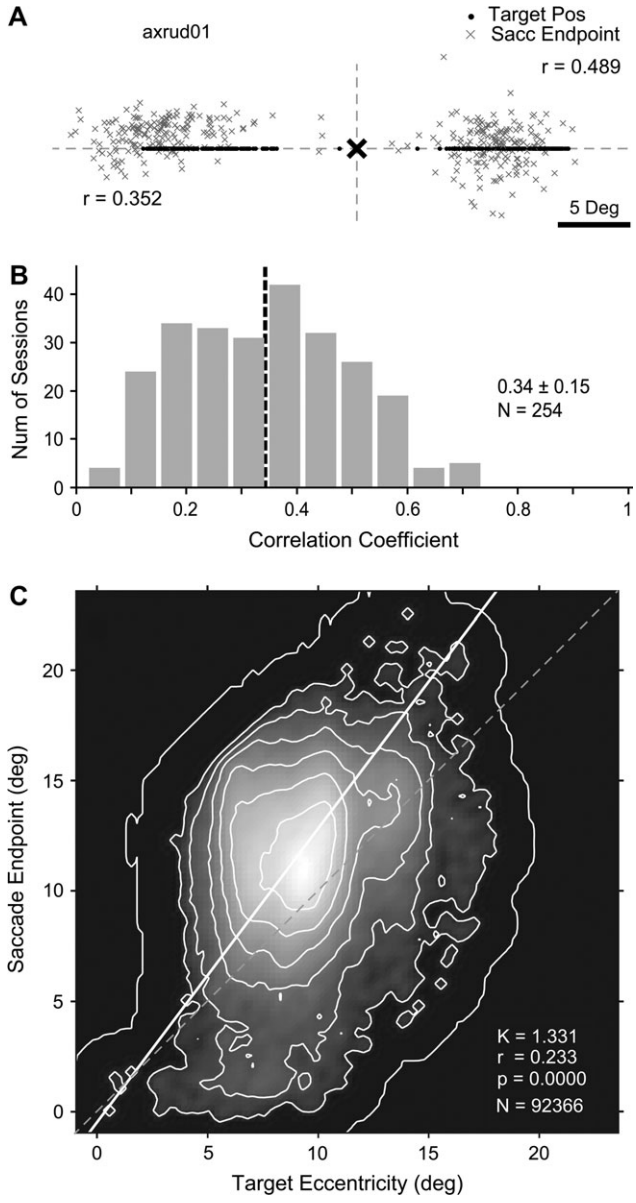

Figure 2. Behavioral performance. (*A*) Sample recording in animal A. It shows correlation between the saccade end points (gray *x*'s) and invisible target position (black dots) when target is moving either toward or away from RF. Numbers are the correlation coefficient between saccade end point and target position for each direction. (*B*) The population distribution of the correlation coefficients for all recordings at both directions. (*C*) Saccade end point versus target eccentricity. Dashed line is $x = y$. Straight white line is best-fit linear regression, K is the slope of the regression line. N is the number of trials, r is the correlation coefficient, and p is the significance level of the correlation.

sum of their x-y coordinates. The data for all recording sites are plotted in Figure 2*C*. Due to the large number of data points (>90,000), the scatterplot was converted to a density map by smoothing the data with a 2D radially symmetric Gaussian filter ($\sigma = 0.25$ degrees). The correlation ($r = 0.23$) between saccade and target eccentricity was weaker than in the 2D correlation of saccade and target position but was still highly significant ($P < 0.0001$). The slope of the regression line was close to unity. There was no significant difference in the correlation values when trials were split into probe versus no-probe (paired *t*-test $P = 0.082$).

Eye Movements during Fixation

It is possible that the probe stimuli would cause bottom–up orienting through automatic capture of attention (see Yantis 1996). The capture of attention might be reflected in eye movements around the time of probe presentation. These might include saccades made toward the probe location or small movements such as slow drifts or microsaccades that remained within the fixation window (Laubrock and others 2005). We did not analyze saccades directed toward the probes because trials were aborted if the monkey broke fixation (i.e., if his eye position moved out of the 2 × 2 fixation window before the GO signal). In general, these fixation breaks occurred when the monkey was tired, satiated, or otherwise unwilling to work. Only a few were due to the monkey making a saccade to the probe. All of the analysis in this study is based on trials in which the monkey did not break fixation. For these trials, we analyzed small eye movements, including microsaccades and slow drifts, by calculating radial eye position and eye velocity around the time of each probe presentation. To do this, we first established a common reference system by rotating the target, probe, and eye position data for all trials onto the x axis such that target movement matches the x axis and is always directed towards positive x values. We then selected the eye position and velocity data within a 175-ms time window around each probe and constructed averages sorted according to whether the probe was to the left or right of fixation. These averages are shown in Figure 3.

The eye position means (Fig. 3*A*) show a small but systematic difference between left and right probe locations (SDs averaged 0.34 degrees, standard errors of mean were smaller than the width of the lines). This small difference (less than 0.005 degrees) was present even before the onset of the probe and was found to be systematically related to the direction of target motion and not an effect of the probe. The main effect of the probe was to cause a deviation of eye position about 80–90 ms after probe onset. These deviations tended to be toward the location of the probe. The same tendency was found for eye velocity (Fig. 3*B*). A 3-way analysis of variance (ANOVA) (factors = monkey, occluded target location at time of probe, and probe location) was used to determine whether these deviations were statistically significant. The independent variable was either eye position or eye velocity averaged within a 25-ms window 87.5–112.5 ms after probe onset. For eye position, all 3 factors were highly significant ($P < 0.0001$). However, for eye velocity, only probe location was significant ($P < 0.0001$), monkey and target direction were not ($P > 0.44$). To quantify the underlying bias in the data, we did the same ANOVA using the data from a different time window, –25 to 0 ms prior to probe onset. For eye position before the probe, there was a significant effect of monkey and target location ($P < 0.01$) but probe location was not significant ($P \geq 0.09$). For eye velocity, only the variance between animals was significant ($P < 0.0001$) not the effects of target or probe location ($P > 0.44$). We conclude that the probes do have an effect on eye position and velocity, likely reflecting covert orienting of attention, and that this effect starts approximately 80–90 ms after probe onset.

Neuronal Response to Visual Probes

As in previous work using occluded targets (Barborica and Ferrera 2003), a substantial proportion of FEF neurons continued firing during the occlusion interval of the PREDMAP task even when there was no target on the screen. A baseline response was computed by averaging the activity across no-probe trials separately for each direction of target motion. To map visual responses, visual probes were flashed at different times within the occlusion interval and at different locations along the target path. These visual probes changed the neurons' firing rate compared with the no-probe trials. The population of 191 neurons showed 2 types of response to the probes; for some neurons, the probes generally increased firing rate, whereas for other neurons firing was decreased below baseline. To demonstrate that visual neurons in FEF actually do respond to task irrelevant stimuli and to provide an estimate of the robustness of this visual response, responses of a typical neuron during the PREDMAP task are shown in Figure 4. Figure 4*A*,*B* shows the raw spike raster and histograms for all probe trials collapsed across probe location. The vertical green line indicates the onset of the occlusion interval. Small red dots indicate the onset of each probe. There were between 1 and 3 probes on each trial and these could occur in any of 7 time intervals, thus giving rise

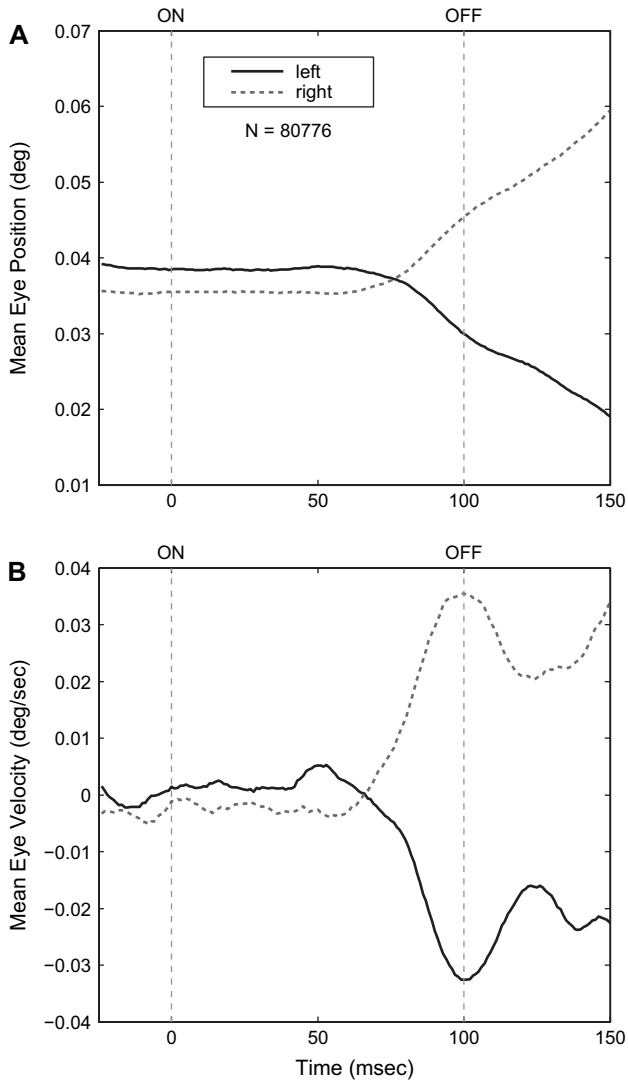

Figure 3. Fixational eye movements in response to probe. (*A*) Average eye position for probes to the left (solid line) and right of fixation (dashed line) (*B*) Average eye velocity sorted by probe location. Vertical dashed lines indicate probe onset and offset times. *N* is the total number of probes in the average.

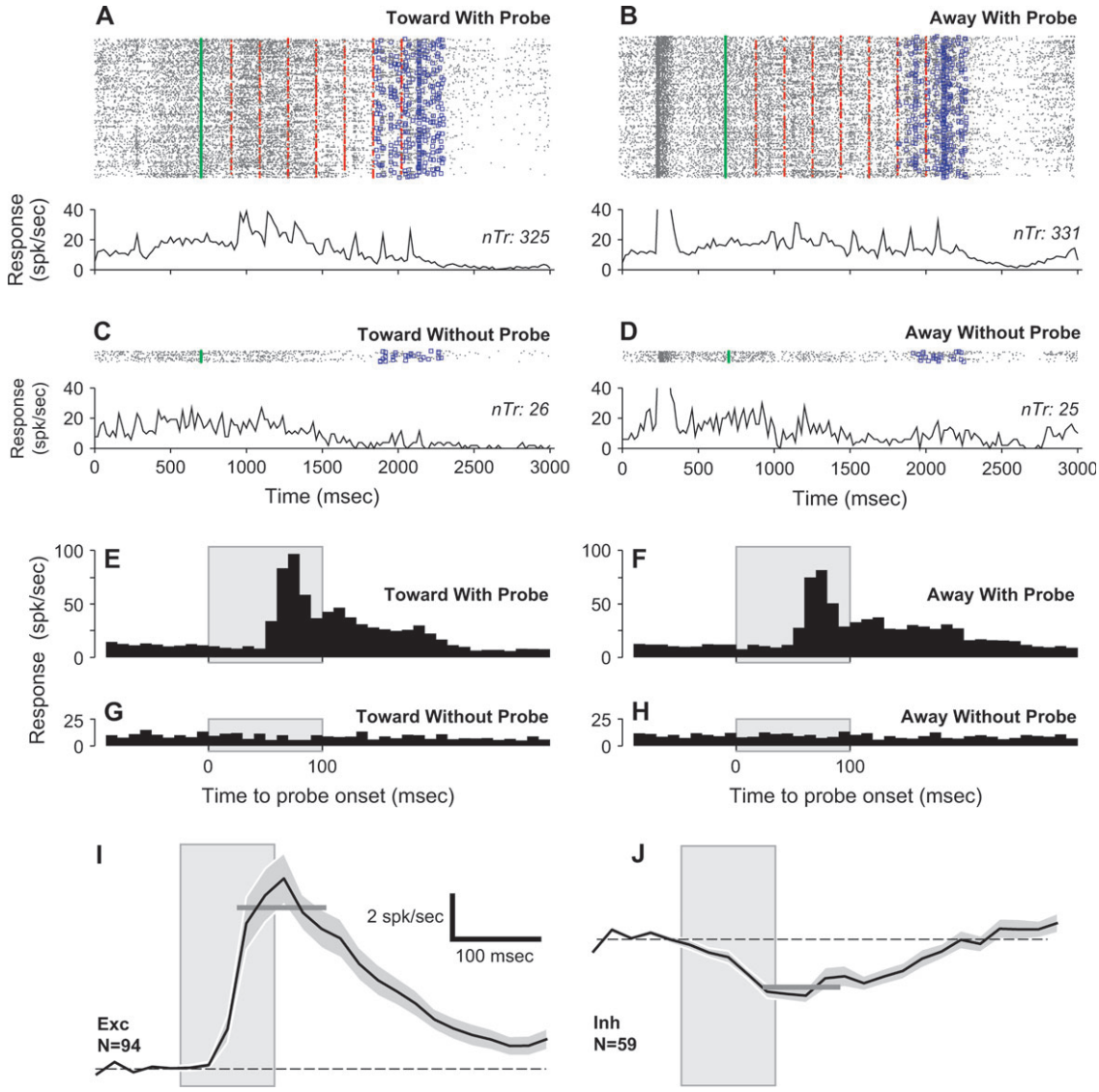

Figure 4. Example neuron response to visual probes. (*A–D*) Raw data of FEF neurons' response. Top: Raster of spikes and events. Bottom: Histogram aligned to the onset of the occlusion interval. (*E–H*) Aligned timestamps to the onset of probes. (*A*, *B*, *E*, and *F*) are trials with probe, (*C*, *D*, *G*, and *H*) are trials without probe. (*A*, *C*, *E*, and *G*) are trials when target is moving toward RF, (*B*, *D*, *F*, and *H*) are trials when target is moving away from RF. (*I*, *J*) Averaged probe response at the population level shows the mean response to visual probe when aligned on probe onset. Background activity of each unit is subtracted in this case before the averaging. We also plot the standard error of the response. (*I*) is averaged response of 94 excited units. (*J*) is averaged response of 59 inhibited units. The gray boxes in (*E–J*) indicate the 100-ms probe window. Dotted lines in (*I*, *J*) indicate the baseline activity. Solid thick lines in (*I*, *J*) are the maximum/minimum responses within the probe response window of excited/inhibited units.

to the 7 peaks in the histogram. The first probe occurred at a minimum of 200 ms after the start of the occlusion interval. Blue squares indicate the GO signal on each trial. Figure 4*C,D* shows trials when there is no probe. Figure 4*E–H* shows response histograms aligned to the onset of each of the corresponding probes.

The population of neurons was divided into 2 classes based on whether the probe response was greater than the baseline (no-probe) activity (excited neurons) or less than the baseline (inhibited neurons). The mean response and standard error of the response profile for different response types are displayed in Figure 4*I,J*. As shown in Figure 4*I*, 94/191 units (49.7%) showed excited visual responses to the probe stimuli. On the other hand, 59/197 units (31%) had activity that was reduced by the appearance of the probe. The terms "excited" and "inhibited" are used here only to describe the responses of the cells and are meant to imply neither that these neurons excite or inhibit other cells nor that they are putative pyramidal neurons or interneurons (Constantinidis and Goldman-Rakic 2002). For the remaining 38/191 (19.9%) units, there was no significant response to the probe. The average latency of the 94 excited units was 70 ms on average, whereas the average latency of the 59 inhibited units was 90 ms relative to probe onset. The average amplitude of the excited response was stronger than the inhibited response, perhaps reflecting the fact that firing rate cannot be reduced below zero.

Spatiotemporal Dynamics of Probe Response

Probe responses were sorted as a function of probe location and onset time and plotted as 2D space–time maps. Figure 5 shows examples of the 2 predominant effects—response enhancement

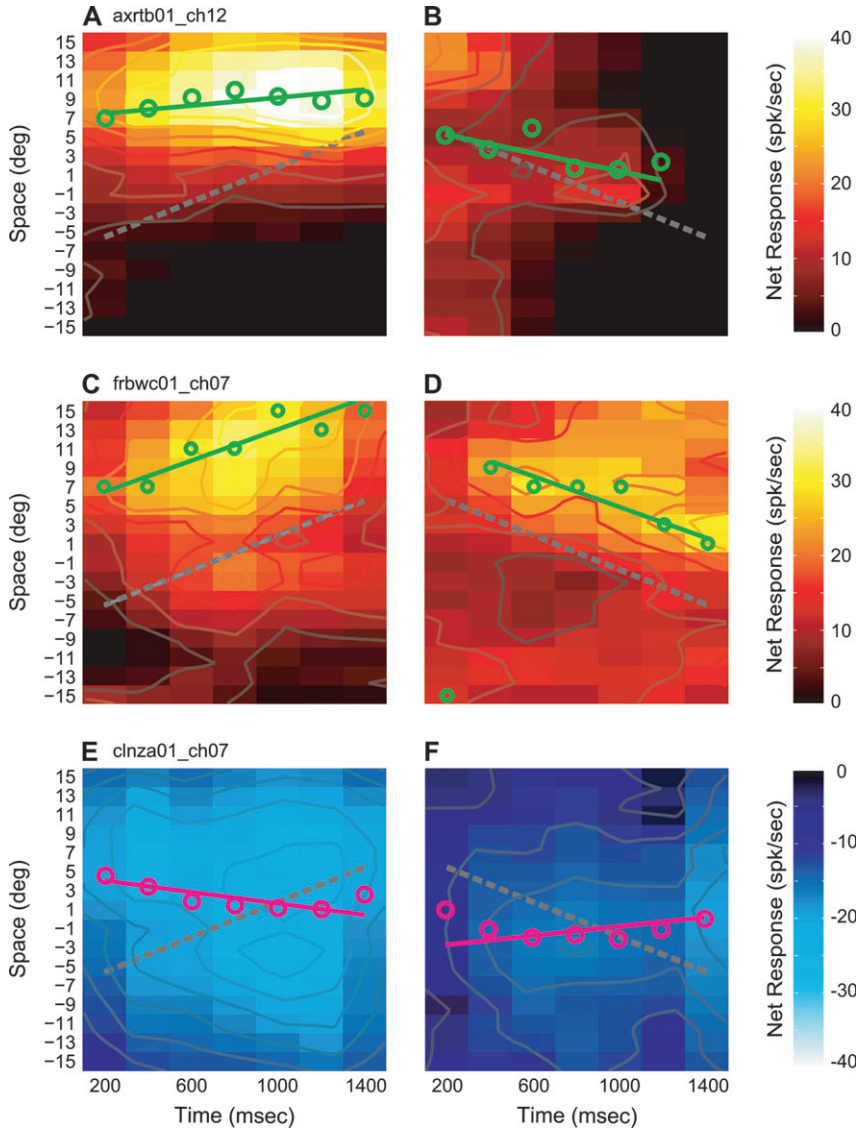

Figure 5. Space–time plots of response to visual probe during the occlusion interval. Net response is defined as the probe–no-probe firing rate. (*A*) Enhancement of response for a single neuron when target moved toward RF. Green circles represent the spatial CMs for each time interval. Green line is best-fitting regression line. Gray dashed line is target position. (*B*) Reduction in response of the same neuron when the target moved away from the RF. (*C*, *D*) Shift in spatial locus of probe response correlated with position of invisible target. Green circles represent the location of the peak probe response in each time interval. Gray dashed line is target position. (*E*, *F*) Neuron that showed a reduction in activity in response to the visual probe. Magenta circles represent the spatial CMs for each time interval. Magenta line is best-fitting regression line. Gray dashed line is target position.

and shifting. What is plotted in the figure is the net response difference between probe trials and no-probe trials. The data were filtered with a 2D (space and time) separable Gaussian filter with space constant σ_x = 3.5 degrees and time constant σ_t = 150 ms. Figure 5*A* shows a neuron that has an enhanced visual response when the target is moving toward the RF (Fig. 5*A*) as compared with the response when the target is moving away from the RF (Fig. 5*B*). The middle panels of Figure 5 show a neuron that had a spatial shift in its response to the probe. When the target was moving toward the RF (Fig. 5*C*), the visual response shifted in that direction. When the target moved away from the RF (Fig. 5*D*), the visual response again shifted in the direction of target motion. Figure 5*E*,*F* shows a neuron whose firing rate was reduced by the probe. In this case, the RF was defined as the region of space in which visual stimuli caused the greatest reduction in response. The reduction in response was greater when the target moved toward the RF (Fig. 5*E*) than when the target moved away (Fig. 5*F*). The cell also showed a slight shift over in the locus of minimal activity and this shift was negatively correlated with target position.

To quantify the shift effect shown in Figure 5, we first calculated the center of mass (CM) for the probe response within each time interval. The (CM) position was obtained by equation (1):

$$\mathrm{CM} = \frac{\sum(s_i * f_i)}{\sum(f_i)}, \qquad (1)$$

where s_i is the probe position in space domain, and f_i is the response (probe – no-probe) averaged over trials with the same probe location. For inhibited cells, f_i is the absolute value of the probe–no-probe difference. The CMs are shown as green or magenta circles in Figure 5 along with the best-fitting regression

lines. As an additional measure, the same analysis was performed using the probe location that gave the maximum response (or minimum for inhibited cells) in each time interval. Figure 5*A,B,E,F* shows the CMs (green or magenta circles), whereas Figure 5*C,D* shows the peak locations. Outliers, such as that shown in the first time interval in Figure 5*D*, were excluded when computing the best-fit regression line. Then, we calculated the correlation coefficient between the position of this CM and the position of invisible target at the corresponding time (Fig. 5, dashed gray lines). For excited cells, 72/91 (79%) showed a significant correlation when target motion was toward the RF. (Note: the total is less than 94 because 3 cells were dropped due to data that were incomplete for this analysis.) For cells that were significantly correlated ($P < 0.05$), the median correlation was $r = 0.32$. For trials with motion away from the RF, 73/92 (79%) excited cells showed a significant correlation and the median was $r = 0.36$. For inhibited neurons, 44/57 (77%) were significantly correlated when motion was toward the RF and the median was $r = -0.64$; when motion was away from the RF, 36/56 (64%) were significantly correlated and the median was $r = 0.29$. In general, the results were more reliable for trials with the target moving toward the RF because these tended to have stronger responses. In these trials, excited cells had probe responses that shifted in the same direction as the target motion, whereas inhibited neurons had responses that shifted opposite to the direction of target motion.

We next quantified the enhancement effect shown in Figure 5*A,B*. Figure 6 shows the enhancement effect at the population level. Enhancement was calculated by averaging the response over all spatial locations, and then comparing this averaged response for "toward" and "away" trials. Figure 6*A* is the difference of averaged response between toward trials and away trials for all neurons, including those with excited response ($n = 94$) and those with inhibited responses ($n = 59$). The difference between toward and away responses was significant at the population level for both groups (paired *t*-test; $P < 0.05$). To estimate the magnitude of the enhancement effect, the data were fit with linear regression (first principal component). For excited units, the response was about 17% stronger when target is moving toward the RF. For inhibited units, the inhibition was about 54% stronger when target moved toward the RF. Figure 6*B,C* shows the distribution of the response differences between the toward trials and away trials. The mean difference was significantly different from zero for both groups of neurons.

This analysis was done by pooling data over all probe locations and times, including locations with weak or negligible responses, and is therefore likely to underestimate the strength of the effect. An analysis that considered only probes within the spatiotemporal RF of each neuron would likely yield stronger effects but would involve the additional complication of choosing a subset of probe locations and responses for each neuron. In fact, one could always choose a subset of the data that showed the "desired" effect. We chose to avoid these complications at the risk of diluting the strength of the effect. However, by making fewer assumptions, the analysis we have performed is more robust.

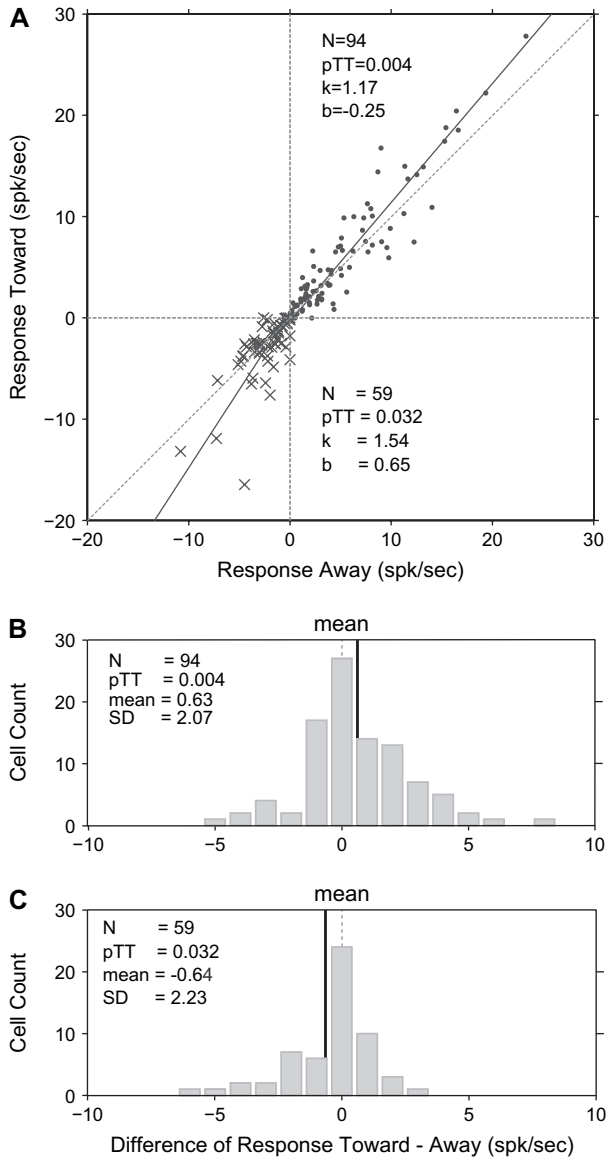

Figure 6. Enhancement effect at population level. (*A*) Black dots represent cells that had excited responses, and black crosses represent cells that had inhibited responses. Dashed line is $x = y$. Solid lines are the linear regression based on the first principal component. The legend indicates the number of cells (*N*), significance of paired *t*-test (pTT), slope (*k*), and intercept (*b*) of regression, when target is moving toward versus away from the RF. (*B*) Distribution of Toward–Away differences for cells with excited responses. (*C*) Same for cells with inhibited responses.

Early versus Late Probe Responses

Because FEF is involved in movement planning, one might expect visual responses to become suppressed as the time for the movement draws near (Powell and Goldberg 2000). To investigate this, we compared the probe response (probe trials – no-probe trials) for probes that were flashed at different times in the occlusion interval (early vs. late). For neurons with excited responses, early probes evoked on average a 27% greater response than late probes (Fig. 7, black dots). This effect was significant at the population level (paired *t*-test; $P < 0.005$). For neurons with inhibited responses, there was no significant effect (Fig. 7, gray dots). These results indicate that the enhancement effect shown in Figure 6 is superimposed on a general decline in visual responsiveness in excited neurons as the time for the movement approaches. However, as Figure 5*A* demonstrates, some neurons had significant probe responses late in the occlusion interval.

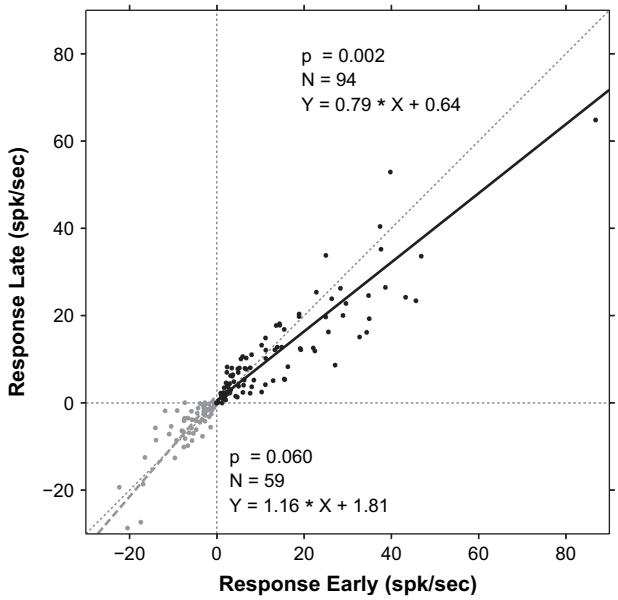

Figure 7. Response to probe presented earlier or later in the occlusion interval. Black dots and solid regression line are for excited units; gray dots and dashed line are for inhibited units. Legend indicates number of cells, *P* value for paired *t*-test, and equation of regression line.

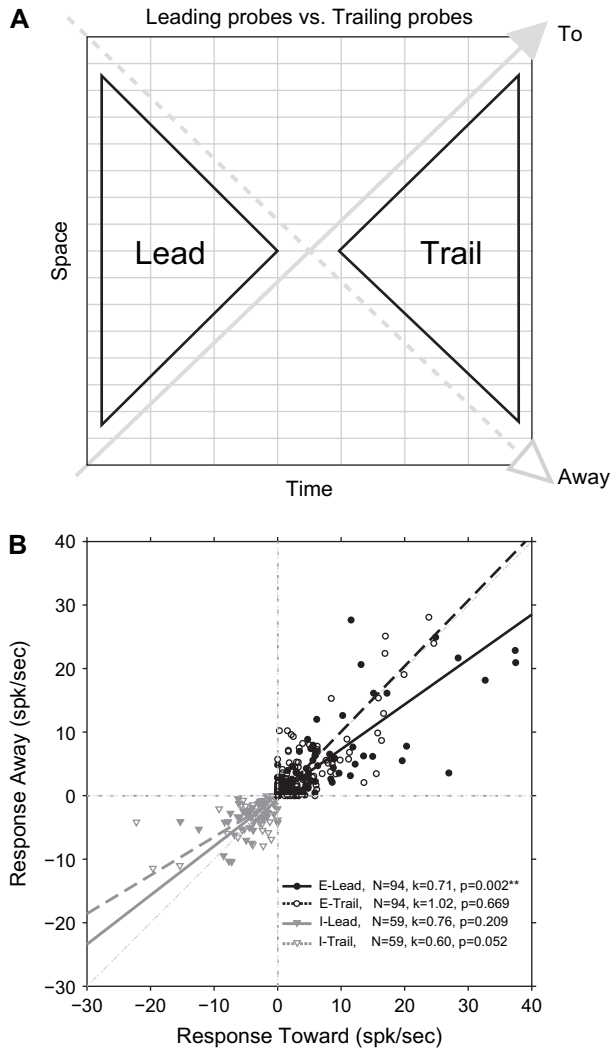

Figure 8. Responses to leading and trailing probes. (*A*) Space–time loci of "leading" and "trailing" probes. (*B*) Responses to leading and trailing probes sorted by target direction relative to RF (toward vs. away). Black circles are data for excited neurons, and gray triangles are for inhibited neurons. The legend gives the number of cells (*N*), slope of the regression line (*k*), and significance level (*P*) of paired *t*-test (toward vs. away).

Leading versus Trailing Probes

If FEF is involved in constructing a predictive representation of target motion, then one might expect an enhancement of responses to probes that lead the target as compared with probes that follow in the wake of the target. Probes with spatial–temporal coordinates located within the left triangle marked as "leading" area in Figure 8*A* always appeared in front of the target regardless of whether the target is moving toward or away from the RF. Probes within the triangular area marked "trailing" always fell behind the moving target. Figure 8*B* compares the average response on toward trials versus away trials. This comparison was made not for all probes but only for those probes with coordinates that fall within the leading condition or trailing condition. The results show that for excited neurons, the probe response was significantly enhanced when the target moved toward the RF, but only for probes that led the target not for those that trailed. For inhibited cells, the probe response tended to inhibit firing more when the target moved away from the RF, and this effect was strongest for trailing probes. These results suggest that excited neurons tend to anticipate the motion of the target; that is, they are more excitable not only when the target is moving toward the RF but also for probe locations ahead of the extrapolated target position. Conversely, inhibited cells show the greatest response reduction in the wake of the invisible target.

Discussion

Visual responses of FEF neurons were modulated during a task that required monkeys to extrapolate the position of an invisible moving target. The effect of visual probes reached its maximum an average of 70 ms delay after probe onset. The probe response could be either greater (excited effect) or smaller (inhibited effect) than activity during the same time interval on interleaved no-probe control trials. Both excited and inhibited probe responses were stronger during trials where the target moved toward the RF than trials where the target moved away. In some neurons, the locus of the visual response shifted over time. For excited neurons, the shift tended to be in the same direction as the target motion, whereas inhibited units tended to show a negative correlation with target motion.

It is likely that the probe responses include both sensory and attentional components. The latency of the probe responses was well under 100 ms, suggesting that the initial response was primarily sensory. However, the later response is probably modulated by attentional capture due to the sudden onset of the probes. Analysis of fixational eye movements shows clear evidence of attentional orienting toward the probe location starting about 80 ms after probe onset. The presence of the probes did not have a significant effect on task performance. It is therefore possible that the responses evoked by the probes were modulated when monkeys endogenously shifted the locus of attention to correspond with the inferred position of the invisible target. These results suggest that FEF plays a role in the

predictive tracking of moving targets and that this role includes a sensory/perceptual component.

Enhancement

One of the main effects found in this study is that probe responses tended to be stronger when the target was moving toward the RF than when the target was moving away from the RF. It is important to note that this is not a preparatory activity. Many FEF neurons have preparatory activity that builds up in anticipation of an eye movement, and this activity is generally stronger for movements toward the RF than for movements away. The probe response represents additional activity that is superimposed on this preparatory activity and reflects the neuron's sensitivity to visual inputs at various locations and time points during the delay interval. For some cells, such as that illustrated in Figure 5*A,B*, the visual response was strongest near the end of the occlusion interval, indicating that visual sensitivity increased as the time for the movement drew nearer. However, at the population level, probe responses were generally strongest early in the occlusion interval. This is similar to the pattern of results found in parietal area LIP = Lateral Intraparietal Area (Powell and Goldberg 2000). One interpretation of this is that movement preparation reduces visual sensitivity in the FEF. A possible mechanism for this is that as preparatory activity increases, the incremental response evoked by the visual probe decreases due to response saturation.

Enhancement of probe responses was greatest when probes were flashed ahead of the extrapolated target position, whereas inhibition was greatest when probes were flashed behind the target. Furthermore, the enhancement effect was found for excited neurons, which were roughly twice as common (n = 94) as inhibited neurons (n = 59). At the population level, the net effect might be an enhanced representation for probes presented ahead of inferred target motion, which might facilitate the production of saccades toward visible as well as invisible targets. A recent study (Blohm and others 2005) showed that when saccades are made to a target flashed during smooth pursuit, saccade latencies are shorter for targets flashed ahead of pursuit relative to targets flashed in the wake of pursuit. This is similar to the observation that saccades made to moving targets are shorter if the target is moving toward the fovea than if the target is moving away (Segraves and others 1987). These effects may be related to the finding that attention tends to be allocated ahead of pursuit targets (van Donkelaar 1999). The shorter latencies found for saccade targets presented ahead of pursuit also extended to targets presented up to 90 degrees from the direction of motion. Although in our experiment we have aligned the direction of movement with the RF location, the size of the RFs as well as the scatter in RF location among neurons at a given recording site makes it possible that the perceptual advantage of leading probes (or saccade targets) extends laterally to significant distances in visual space, consistent with the findings of Blohm and others (2005). At the same time, the backward propagation of a wave of inhibition may explain longer latencies for saccadic targets presented behind the pursuit target. The perceptual disadvantage of trailing probes may be related to the "inhibition of return" phenomenon, where previously attended locations (in our case those lying on the occluded target trail, behind its current position) are known to be at a competitive disadvantage with respect to new ones (for a review, see Klein 2000).

Shifting

Shifting RFs have been described previously in FEF (Umeno and Goldberg 1997), LIP (Duhamel and others 1992; Colby and Goldberg 1999), and V4 (Connor and others 1997) during tasks that involved spatial attention and/or preparation of saccadic eye movements. In V4, the visual response shifted toward the attended location. This is consistent with the idea that shifting RFs in FEF reflect the deployment of attention along the target path during predictive saccades to invisible moving targets. The shifts that have been described previously in LIP and FEF were closely coupled in time to the production of saccades and may reflect a mechanism for predictively updating a representation of space in prefrontal cortex in advance of eye movements. The shifting visual responses found in the current study occurred hundreds of milliseconds before the saccade and may reflect a different predictive mechanism; one that represents the motion of a specific visual stimulus rather than updating the entire visual scene (Heiser and Colby 2006).

One seemingly mysterious aspect of the current results is that, whereas neurons with excited probe responses tend to shift in the direction of target motion, neurons with inhibited responses tend to shift in the opposite direction. This effect makes sense if one assumes that neurons in FEF have an inhibited effect on neurons that represent different spatial locations or saccade vectors. This inhibitory scheme is supported by studies of the effect of electrical stimulation in FEF (Burman and Bruce 1997) and also by neuronal recording studies showing that the firing of some FEF neurons is correlated with the inhibition of saccades (Hasegawa and others 2004). Thus, as a target moved across the spatial map in FEF, it would be preceded by a wave of excitation along the target trajectory, whereas at the same time a wave of inhibition would start near the end point of the trajectory and move in the opposite direction. This inhibited scheme might help keep the excited wave moving in one direction rather than spreading out in all directions. It might also help focus the spread of excitation when the target is invisible, thereby maintaining the "perceptual momentum" (Freyd and Finke 1984; Kelly and Freyd 1987) in the absence of a visible target.

Relationship to Previous Work

Several elegant experiments conducted by Assad and colleagues have established that parietal cortex plays a role in inferring the motion of occluded targets (Assad and Maunsell 1995) and have also distinguished between sensory and motor components of the prediction mechanism in parietal areas MST = Medial Superior Temporal Area, LIP = Lateral Intraparietal Area, and MIP = Medial Intraparietal Area (Eskandar and Assad 1999, 2002). In these studies, monkeys made manual responses using a joystick, whereas in the current experiments eye movements were the response modality. One conclusion of Eskandar and Assad (1999) was that the visual and motor components of the task were represented in different parietal areas. The results of the present study along with previous work in our lab (Barborica and Ferrera 2004) suggest that for predictive saccades, FEF may represent both the sensory and motor aspects of the behavior.

FEF has been shown to play a role in predictive smooth pursuit eye movements (see Keating 1991; Fukushima and others 2004), although predictive behavior can be observed after ablation of FEF (Keating 1993). These predictive responses were found in the smooth pursuit subregion of the FEF. In the

current study, recordings were not made at any sites where electrical microstimulation evoked smooth eye movements.

Saccades also show predictive behavior in response to moving targets. For example, studies have found that saccades are programmed based on an estimate of target position taken some 100 ms prior to the initiation of the movement (Gellman and Carl 1991). For an object moving at a moderate speed, this delay could cause the eye to undershoot the target. Yet, saccades made to moving targets are accurate because their programming includes a predictive component that compensates for the velocity of the target (Ron and others 1989; Keller and Johnsen 1990). These predictions require an intact striate cortex (Segraves and others 1987) and therefore appear to depend on cortical motion processing.

The current study as well as previous work from our lab (Barborica and Ferrera 2003, 2004) and others (Bennett and Barnes 2006; Orban de Xivry and others 2006) have tested the limits of oculomotor prediction when the target is rendered temporarily invisible. This is a situation that occurs naturally when a moving object is occluded by another object. The ability to predict the motion of the occluded target may depend on maintaining an internal representation of the invisible target and continuously updating that representation to provide an estimate of target position at each moment in time. This ability may reflect a dynamic aspect of spatial working memory that plays a role in navigating a complex environment that contains moving objects constantly coming into or out of view.

Notes

This work was supported by NIH-MH59244 and the Whitehall Foundation. *Conflict of Interest*: None declared.

Address correspondence to email: vpf3@columbia.edu.

References

Assad JA, Maunsell JH. 1995. Neuronal correlates of inferred motion in primate posterior parietal cortex. Nature 373(6514):518–521.

Barborica A, Ferrera VP. 2003. Estimating invisible target speed from neuronal activity in monkey frontal eye field. Nat Neurosci 6(1):66–74.

Barborica A, Ferrera VP. 2004. Modification of saccades evoked by stimulation of frontal eye field during invisible target tracking. J Neurosci 24(13):3260–3267.

Bennett SJ, Barnes GR. 2006. Combined smooth and saccadic ocular pursuit during the transient occlusion of a moving visual object. Exp Brain Res 168(3):313–321.

Blohm G, Missal M, Lefevre P. 2005. Processing of retinal and extraretinal signals for memory-guided saccades during smooth pursuit. J Neurophysiol 93(3):1510–1522.

Bruce CJ, Goldberg ME. 1985. Primate frontal eye fields. I. Single neurons discharging before saccades. J Neurophysiol 53(3):603–635.

Bruce CJ, Goldberg ME, Bushnell MC, Stanton GB. 1985. Primate frontal eye fields. II. Physiological and anatomical correlates of electrically evoked eye movements. J Neurophysiol 54(3):714–734.

Burman DD, Bruce CJ. 1997. Suppression of task-related saccades by electrical stimulation in the primate's frontal eye field. J Neurophysiol 77(5):2252–2267.

Churchland MM, Chou IH, Lisberger SG. 2003. Evidence for object permanence in the smooth-pursuit eye movements of monkeys. J Neurophysiol 90(4):2205–2218.

Colby CL, Goldberg ME. 1999. Space and attention in parietal cortex. Annu Rev Neurosci 22:319–349. [Review].

Connor CE, Preddie DC, Gallant JL, Van Essen DC. 1997. Spatial attention effects in macaque area V4. J Neurosci 17(9):3201–3214.

Constantinidis C, Goldman-Rakic PS. 2002. Correlated discharges among putative pyramidal neurons and interneurons in the primate prefrontal cortex. J Neurophysiol 88(6):3487–3497.

Duhamel JR, Colby CL, Goldberg ME. 1992. The updating of the representation of visual space in parietal cortex by intended eye movements. Science 255(5040):90–92.

Eskandar EN, Assad JA. 1999. Dissociation of visual, motor and predictive signals in parietal cortex during visual guidance. Nat Neurosci 2(1):88–93.

Eskandar EN, Assad JA. 2002. Distinct nature of directional signals among parietal cortical areas during visual guidance. J Neurophysiol 88(4):1777–1790.

Ferrier D. 1876. The functions of the brain. London: Smith, Elder & Co.

Filion CM, Washburn DA, Gulledge JP. 1996. Can monkeys (*Macaca mulatta*) represent invisible displacement? J Comp Psychol 110:386–395.

Freyd JJ, Finke RA. 1984. Representational momentum. J Exp Psychol Learn Mem Cogn 10:126–132.

Fukushima K, Yamanobe T, Shinmei Y, Fukushima J, Kurkin S. 2004. Role of the frontal eye fields in smooth-gaze tracking. Prog Brain Res 143:391–401.

Funahashi S, Bruce CJ, Goldman-Rakic PS. 1989. Mnemonic coding of visual space in the monkey's dorsolateral prefrontal cortex. J Neurophysiol 61(2):331–349.

Gellman RS, Carl JR. 1991. Motion processing for saccadic eye movements in humans. Exp Brain Res 84(3):660–667.

Goldberg ME, Bruce CJ.1990. Primate frontal eye fields. III. Maintenance of a spatially accurate saccade signal. J Neurophysiol 64(2): 489–508.

Goldberg ME, Bushnell MC. 1981. Behavioral enhancement of visual responses in monkey cerebral cortex. II. Modulation in frontal eye fields specifically related to saccades. J Neurophysiol 46(4): 773–787.

Goldman-Rakic PS, Selemon LD. 1997. Functional and anatomical aspects of prefrontal pathology in schizophrenia. Schizophr Bull 23(3):437–458.

Hasegawa RP, Peterson BW, Goldberg ME. 2004. Prefrontal neurons coding suppression of specific saccades. Neuron 43(3):415–425.

Heiser LM, Colby CL. 2006. Spatial updating in area LIP is independent of saccade direction. J Neurophysiol 90(5):2751–2767.

Hooker C, Park S. 2000. Trajectory estimation in schizophrenia. Schizophr Res 45:83–92.

Judge SJ, Richmond BJ, Chu FC. 1980. Implantation of magnetic search coils for measurement of eye position: an improved method. Vision Res 20(6):535–538.

Keating EG. 1991. Frontal eye field lesions impair predictive and visually-guided pursuit eye movements. Exp Brain Res 86(2): 311–323.

Keating EG. 1993. Lesions of the frontal eye field impair pursuit eye movements, but preserve the predictions driving them. Behav Brain Res 53(1–2):91–104.

Keller E, Johnsen SD. 1990. Velocity prediction in corrective saccades during smooth-pursuit eye movements in monkey. Exp Brain Res 80(3):525–531.

Kelly MH, Freyd JJ. 1987. Explorations of representational momentum. Cogn Psychol 19(3):369–401.

Klein WM. 2000. Inhibition of return. Trends Cogn Sci 4(4):138–147.

Laubrock J, Engbert R, Kliegl R. 2005. Microsaccade dynamics during covert attention. Vision Res 45(6):721–730.

Moore T, Armstrong KM, Fallah M. 2003. Visuomotor origins of covert spatial attention. Neuron 40(4):671–683.

Moore T, Fallah M. 2001. Control of eye movements and spatial attention. Proc Natl Acad Sci USA 98(3):1273–1276.

Opris I, Barborica A, Ferrera VP. 2001. On the gap effect for saccades evoked by electrical microstimulation of frontal eye fields in monkeys. Exp Brain Res 138(1):1–7.

Opris I, Barborica A, Ferrera VP. 2005. Effects of electrical microstimulation in monkey frontal eye field on saccades to remembered targets. Vision Res 45(27):3414–3429.

Orban de Xivry JJ, Bennett SJ, Lefevre P, Barnes GR. 2006. Evidence for synergy between saccades and smooth pursuit during transient target disappearance. J Neurophysiol 95(1):418–427.

Pavel M, Cunningham H, Stone V. 1992. Extrapolation of linear motion. Vision Res 32:2177–2186.

Paxinos G, Huang X-F, Toga AW. 2000. The rhesus monkey brain in stereotaxic coordinates. Academic Press, San Diego, CA.
Piaget J. 1954. The construction of reality in the child. New York: Basic Books.
Posner MI, Petersen SE. 1990. The attention system of the human brain. Annu Rev Neurosci 13:25–42.
Powell KD, Goldberg ME. 2000. Response of neurons in the lateral intraparietal area to a distractor flashed during the delay period of a memory-guided saccade. J Neurophysiol 84(1): 301–310.
Ron S, Vieville T, Droulez J. 1989. Target velocity based prediction in saccadic vector programming. Vision Res 29(9):1103–1114.
Rosenbaum DA. 1975. Perception and extrapolation of velocity and acceleration. J Exp Psychol Hum Percept Perform 1(4): 395–403.
Segraves MA, Goldberg ME, Deng SY, Bruce CJ, Ungerleider LG, Mishkin M. 1987. The role of striate cortex in the guidance of eye movements in the monkey. J Neurosci 7(10):3040–3058.
Umeno MM, Goldberg ME. 1997. Spatial processing in the monkey frontal eye field. I. Predictive visual responses. J Neurophysiol 78(3):1373–1383.
van Donkelaar P. 1999. Spatiotemporal modulation of attention during smooth pursuit eye movements. Neuroreport 10(12):2523–2526.
Watson JS, Gergely G, Csanyi V, Topal J, Gasci M, Sarkozi Z. 2001. Distinguishing logica from association in the solution of an invisible displacement task by children (*Homo sapiens*) and dogs (*Canis familiaris*): using negation of disjunction. J Comp Psychol 115:219–226.
Yantis S. 1996. Attentional capture in vision. Washington DC: American Psychological Association.